

Review on Novel Methods used for the Real Time Surveilling of Metal Additive Manufacturing

Shine George

Lecturer
Automobile Engineering
Technical Education Department, Kerala
Government Polytechnic College, Kalamassery, India

Abstract- In this article, the state of the art uses of artificial intelligence (AI) in the Powder Bed Fusion (PBF) field are discussed. PBF is a unique Additive Manufacturing(AM) technique for making critical small-sized complex geometrical parts in medical and aerospace applications from hard to process materials. Process repeatability, quality control, and minimum cost can be attained only through minimizing the in-process defects. In situ determination of the process, defects are vital in attaining high productivity as well as low cost. Lack of information about the physical phenomena happening in the depth of the material mass during the process limits its usage within a narrow spectrum of applications. A variety of AI algorithms can be seen in recent literature which will help to identify process-structure-property-performance (PSPP) relationships in AM. The performance characteristics and challenges of various AI algorithms in this regard are reviewed here.

Index Terms- Powder Bed Fusion; In-situ monitoring; Real-time monitoring; Artificial intelligence.

I. INTRODUCTION

Additive manufacturing (AM) with Powder Bed Fusion (PBF) is apposite for the production of metallic components with complex geometry and elaborate internal features and that is why aerospace and energy industries have adopted this to produce parts of aircraft engines and gas turbines. PBF has tremendous potential in overcoming the existing obstacles of traditional manufacturing such as mass customization and manufacturing lead time. It has been proved by recent studies in the aerospace industry that the PBF process can considerably reduce the buy-to-fly ratio, which is the ratio between the weight of the material required to make a part of the final weight of the finished part. For metal AM, a lesser ratio of 2:1 can be attained compared to a ratio of 20:1 for conventional subtractive processes. Similarly, the lead time for delivering a new part design can be shortened to 1/20th than that of traditional one [1]. This unique flexibility in the design and production of metal AM has the high potential to revolutionize tactical industries, such as aerospace and biomedical. Also, this process is suitable for making parts from hard-to-process materials, such as cobalt-chrome and nickel-based super alloys. Classification of metal AM as per ASTM F42 is depicted in Fig.1. According to ASTM designation: F2792 – 12a for PBF, it is an additive manufacturing process in which heat energy selectively fuses regions of a powder bed. The unexpected phenomena of powder spreading and melt-pool dynamics during PBF cause imperfections in the part which act to degenerate the part quality and mechanical properties. Therefore, the in-situ process monitoring is a hopeful yet challenging means of non- destructive testing. At the very instant that these quality problems happen could be recognized by in-situ or real-time analysis of melt-pool images. In-process assessment for Metal AM is becoming increasingly vital to assure the integrity of parts created in this way.

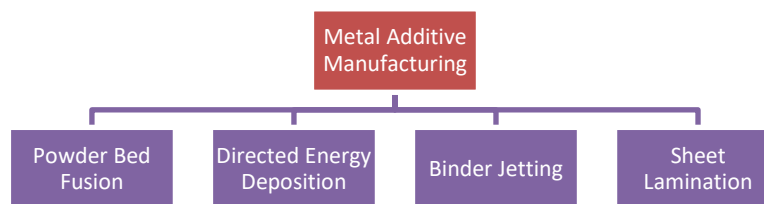


Fig.1. Classification of metal AM as per ASTM F42

II. Factors detrimental to the quality and reliability of the PBF product.

The defects in the PBF process is the result of complex and inter-dependent phenomena, such as absorption and transmission of thermal energy, thermomechanical properties of the material, multi-scale solidification phenomena of powder feedstock, complicated and dissimilar microstructural evolution, capillarity and surface tension in the molten pool and materials evaporation [2]. Therefore, to achieve the desired quality and reliability in the AM product the printing environments should be closely controlled. The contributing parameters will be discussed in the next section. In this section, we will discuss the various defects that are common in metal AM products. In process defects in PBF are classified into seven types. They are porosity, cracking, balling, delamination, warping, residual stresses, and geometric deviations [3,4,5,6,7,8].

a. *Porosity*

Porosity is common in PBF systems and can be mainly of two types: Lack of fusion porosity and porosity due to the presence of gases.

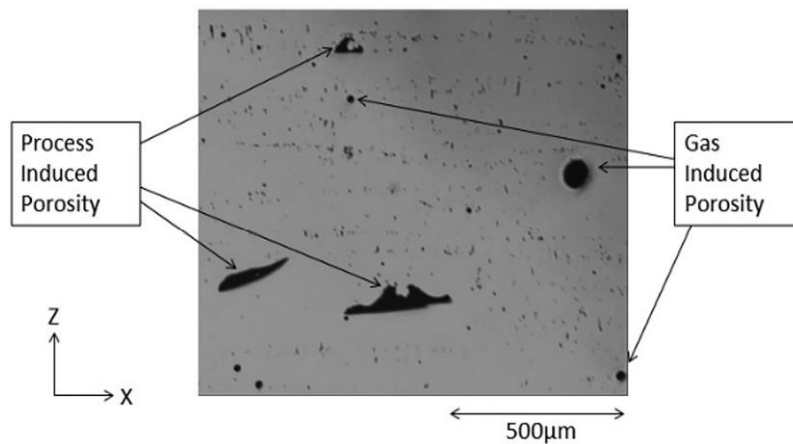


Fig. 2. Gas and Process Induced Porosities.

Lack-of-fusion porosity comes under the process-induced defects category and it is due to insufficient melting of powder, and gas porosity is induced from poor powder feedstock depicted in Fig. 2. Process induced porosities are formed when the thermal energy applied is insufficient to melt the powder or when there is an occurrence of spatter ejection. They are normally non-spherical and appears in different sizes from sub sub-micron to micron. [7]. The presence of porosity in PBF products has a unfavorable consequence on the mechanical properties such as hardness, tensile strength, and fatigue resistance. The machine components fabricated using PBF have significantly lower fatigue resistance than those manufactured using conventional methods due to porosity [7]. The porosity also causes an increase in fatigue crack propagation.

b. Cracking

Parting of solidified metal on the surface or grain boundaries as a result of high-temperature gradient and residual stress [4]. Microstructural images on the cross-sections of Selective Laser Melting (SLM) products printed with different energy levels are shown in Fig. 3.

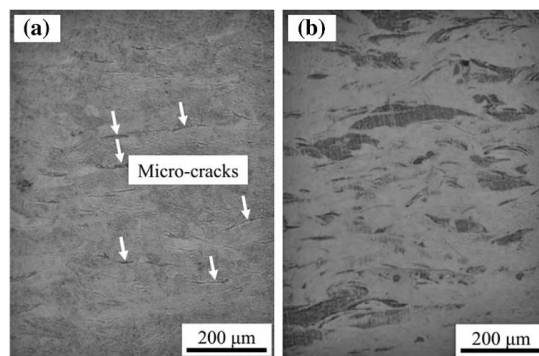


Fig. 3. (a) Micro-Cracks due to high energy (b) Defect-free due to apt energy input

c. Balling

Solidification of molten metal into spheres due to instability in the melt pool surface tension, and wetting dynamics. Balling severities [5] with different scan speeds are shown in Fig. 4

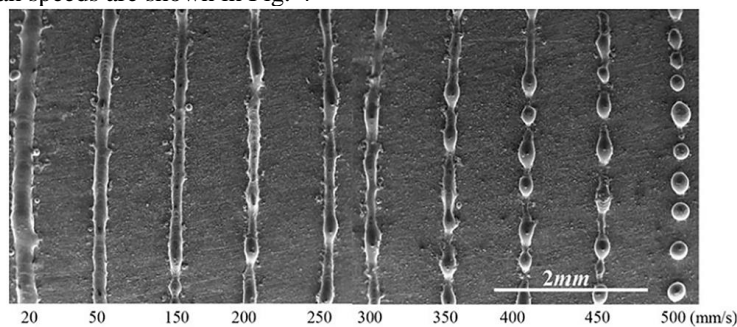


Fig. 4. Balling severities at various speeds

d. Delamination

Separation of successive layers because of insufficient overlap with previous underlying solidified layers, and incomplete melting of the powder particles. Fig. 5 shows an example of serious delamination in SLM parts.

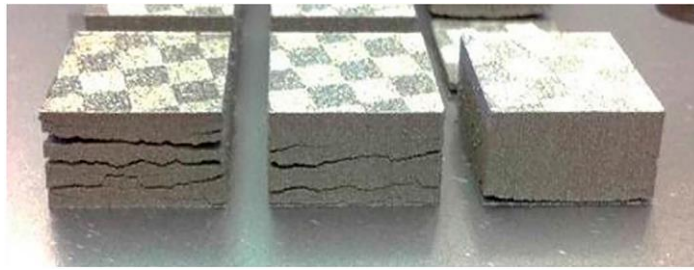


Fig. 5. Layer Delamination

e. Warping

Bending on the sides of the part when the thermal stress in the substrate exceeds the strength of the substrate material. The effect of substrate warping can lead to lack-of-fusion or delamination. Fig. 6 shows the schematic of build plate warping and resultant damage [7].

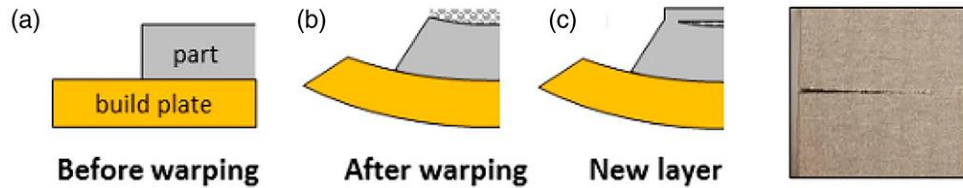


Fig. 6. (a) Before Warping; (b)After Warping; (c) New Layer; (d)Resultant Damage

f. Residual stress

Residual stress is common in metal AM materials due to large thermal gradients during processing, and it can negatively impact mechanical properties and act as a driving force for changes in grain structure. Residual stress is stress within a material that persists after the removal of applied stress. If this stress goes beyond the local yield stress of the material, warping or plastic deformation may occur. If this stress surpasses the local ultimate tensile strength of the material, cracking or other defects may occur [7].

g. Geometric Deviations.

Shrinkage of the molten metal, wrong supports, distortion, and poor calibration of the machine are the causes of geometric deviations from the nominal model [5]. Two common types are given in Fig. 7.

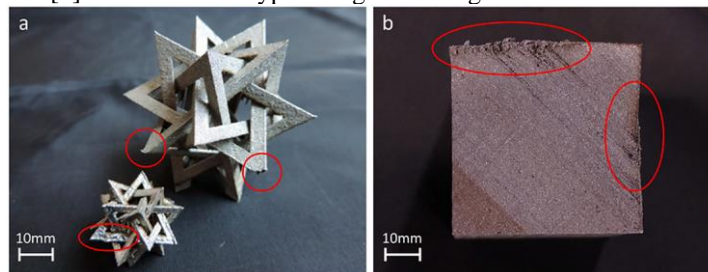


Fig.7. (a) Geometric deviations due to over-hang acute corners; (b) wrongly supported sides.

I. Process Parameters Influencing the Formation of Defects

We can find many defect contributing parameters or factors in recent literature. The most prominent among them are chosen for this review. Malekipour et al [3] broadly classified them into three different types such as Pre- Processed Parameters, Controllable Parameters, and Post-Processed Parameters. Pre-Processed Parameters are again classified into Pre-Defined Parameters and Pre- Defined Parameters to be monitored.

Table 1. Process parameters

Process Parameters - Malekipour et al [3]			Process Factors - Zhang et al [4]		
Pre-processed Parameters	Parameter	Powder Specifications	Powder-related	Powder size	
		Machine Specifications		Powder morphology	
				Gas flow rate	Powder bed density
				Spot size or laser beam radius	Layer thickness
				Laser mode(pulse/continuous wave)	Material properties
				Laser pulse length	
	Building direction				
Parameter	Chamber temperature and powder bed temperature	Temperature-related	Powder bed temperature		

Controllable Parameters	Chamber Conditions	Temperature uniformly in the chamber	Powder feeder temperature	
		Chamber pressure	Temperature uniformity	
		Contained gas of the chamber		
	Laser Specifications	Laser position error	Laser-related	Laser Wavelength
		Platform movement error		Laser Type
		Surface of rolling or blade edge		Laser Power
	Scan Strategy	Laser power	Scan-related	Laser Spot size
		Laser Scanning speed		Hatch spacing
		Hatch spacing		Scan speed
	Manufacturing Specifications	Scan length		Scan strategy
Scan pattern & Scan direction				
	Layer thickness resolution			
	Substrate temperature			

The Controllable Parameters that can be controlled on the fly are seven types. Pre-Defined Parameters and Pre-Defined Parameters Need to be Monitored are eighteen in number. Post-Processed Parameters are mechanical properties and cannot be controlled in real-time. Zhang et al [4] broadly classify those parameters into four types such as Powder Related, Temperature Related, Laser Related, and Scan Related factors and their total number is fifteen. Altogether there are around thirty-three process parameters or factors. Among them, 27 parameters can be monitored and closely controlled [2,3] before or during the PBF process and are given in Table 1.

IV. Review on in-situ and layer wise data acquisition techniques and analytical methods to process those data of irregularities in PBF

A survey on in-situ and layer-wise data acquisition of irregularities and suitable analysis methods to process those are presented in this section. Table 2 shows the parameter or combination of parameters determining the formation of irregularities in PBF and with the citations shown in each cell, we get the various types of data collected and the corresponding analysis techniques from Table 3. A brief discussion of each literature reviewed follows Table 3.

Table 2. Mapping of Irregularities in PBF with Process Parameters and Analytical Methods to Monitor and Control Them.

Irregularities → Parameters	Ballin g	Cracki ng	Gas Porosit y	Lack of Fusion Porosit y Count	Lack of Fusion Porosit y Size	Lack of Fusion Porosit y Locati on	Surfac e Rough ness	Delam ination	Materi al Cross-Contam inati on	Distort ion
Laser Power	[9],[15]	[10][16]		[9],[10] [11][16]	[9],[10] [11][16]	[11]	[10]	[10][16]		
Scan Velocity	[9],[15]	[10]		[9],[10] [11][1]	[9],[10] [11],[1]	[11]	[10]	[10]		
Hatch Spacing	[9]	[10]		[9],[10] [11]	[9],[10] [11]	[11]	[10]	[10]		
Laser Diameter		[10]		[10]			[10]	[10]		
Layer Thickness		[10]		[10]			[10]	[10]		
Machine Specifications	[12]	[12]	[12]	[12]	[12]	[12]	[12]	[12]		

Powder Feed Stock Quality									[13]	
Inaccurate Purging in Machine Set-Up									[13]	
Thermal Conductivity of Powder Bed							[14]			[14]

Table 3. Data types and analysis techniques

Ref. No	Type of Data Collected	Analysis Techniques
[1]	Acoustic Signals	Reinforcement Learning
[9]	CT Scan Image	Multifractal analysis and Hotelling T ² Statistical Control Chart
[10]	Acoustic Signals	Deep Belief Network (DBN)
[11]	X-ray computed tomography Image	Machine Learning with Multifractal analysis
[12]	Layer Wise Optical Images	Constrained Markov Decision Process (CMDP)
[13]	Photodetector Sensor Images	Spectral Graph-Theoretic Approach and Hotelling T ² Statistical Control Chart
[14]	Simultaneous Images from Three Different Sensors	Eigen Spectrum of the Spectral Graph Laplacian Matrix and F-Score
[15]	Raw Image Data	Hybrid Convolutional Neural Networks (CNNs)
[16]	Analyze (Optical) Melt-Pool Image	A regression model with Deep Neural Network (DNN)

Wasmer et al [1] have combined acoustic emission and Reinforcement Learning (RL) for in situ and real-time quality monitoring of PBF. The process parameters were so chosen as to achieve three levels of quality in relation to porosity concentration during the production of a cuboid-shaped stainless steel 316L model with varying laser scan speeds. The acoustic emission (AE) signals were recorded throughout the entire manufacturing process using a Fibre Bragg Grating (FBG) sensor. The AE signals recorded during the AM process were classified based on the quality level depicted in Fig. 8 and in this Fig., left to right, (left) typical light microscope cross-sectional images, (middle) them corresponding AE signals with a 160 ms time, and (right) their corresponding wavelet spectrogram of the areas produced with (a) 300 mm/s, 132 mm³ (medium quality), (b) 500 mm/s, 79 mm³ (high quality) and (c) 800 mm/s, 50 mm³ (poor quality).

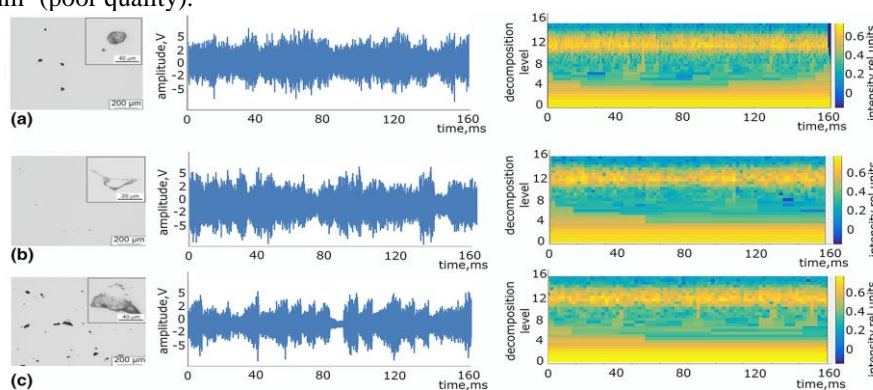


Fig. 8. Spectrogram of the regions produced with (a) medium quality; (b) high quality; (c) poor quality.

The extracted AE wavelet spectrograms were the direct input to the RL algorithm. The original total dataset (training + test dataset) included a total of 180 spectrograms that were equally distributed between each of the three quality classes. After training of the RL-based algorithm, the classification of the porosity concentration quality was performed with a confidence level between 74 and 82%.

Yao et al [9] have proposed a multifractal analysis of layer-wise CT –scan image profiles to detect three types of defects such as balling, cracking, or porosity. In this analysis images of each layer obtained during AM, processes are quantified into three categories such as rough, sinusoidal, and random variations based on the roughness and nonlinearity depicted in Fig. 9.

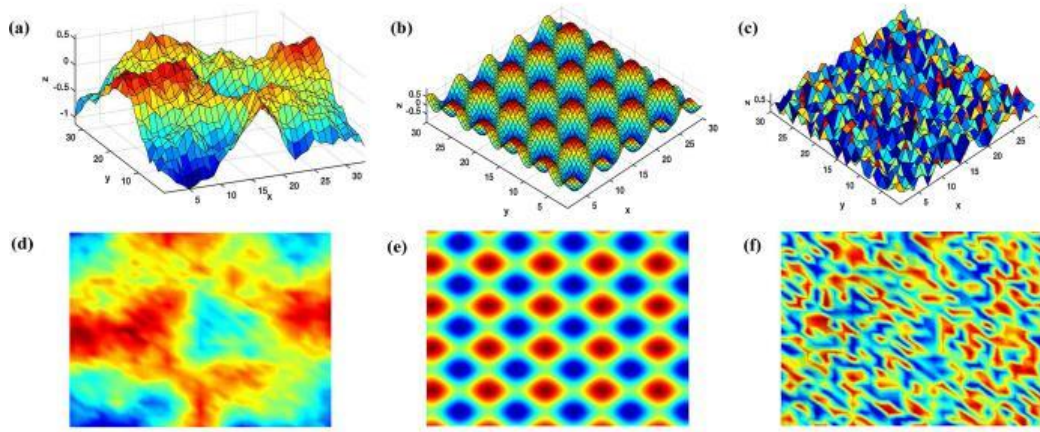


Fig. 9. (a) CT Scan image of rough; (b) sinusoidal; (c) random variations (d); (e); (f) are respectively the 2D images

The local variations in the image data are then characterized by the multifractal spectrum is given in Fig. 10. As the next step, Hotelling T^2 statistics are extracted from the multifractal spectrum for the identification and classification of defects in AM images.

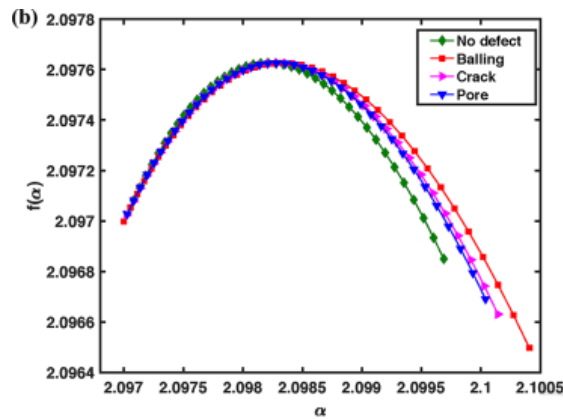


Fig. 10. Multifractal Spectrum

Also, they examined the effect of PBF process parameters such as laser power, scan velocity, and hatch spacing on the multifractal characterization results of defect patterns in AM image contours. Among them, laser power yields the most significant impact on multifractal characteristics than the scan velocity and hatch spacing. They claimed, the multifractal method successfully characterizes and senses the defects in layer-wise AM image profiles. The information thus obtained can be then used for the effective process monitoring and quality control of Laser Powder Bed Fusion (L-PBF).

Ye et al [10] have investigated training Deep Belief Network with acoustic signals obtained from a microphone for quality monitoring of the Selective Laser Melting (SLM) process. The critical quality issues or defects addressed here are porosity, crack, delamination, and surface roughness. Molten states are relative to the energy density E input into the powder, which is inversely proportional to the scanning speed S , laser diameter D , layer thickness T , hatch distance H , and directly proportional to laser power P . All the serious problems such as Cracks and Delamination are the result of balling or overheating. The formation of slight balling, balling, normal, slight overheating, and overheating depicted in Fig. 11 can be distinguished by the DBN algorithm.

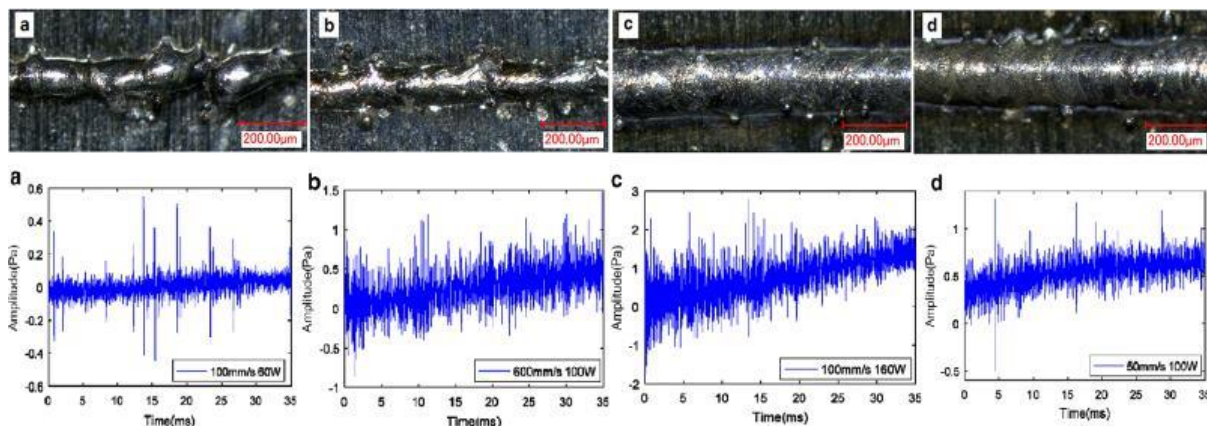


Fig. 11. (a) balling; (b) slight balling; (c) slight overheating; (d) overheating and below shown their corresponding acoustic signals

They claim that the acoustic signal detection method has an advantage over photodiode applications as the SLM process setup greatly hinders the vision in the case of later. Throughout the SLM processing, there exists a melting pool, plasma, and spatter. Quicker speed, higher recognition accuracy, and fewer computation amounts are required in the in situ monitoring processes. Acoustic signals have relationships with the track formation during the SLM process since the formation and acoustic signals are both connected with the plasma variation. The acoustic method detected the defect with fewer data collected from a flexible setup. Acoustic signals were gathered from five defect patterns and used for defect identification by the DBN method. The DBN method extracted the high hierarchical information and connection from the raw acoustic signals, which avoided feature extractions and data pre-processing. They also made a comparison with popular machine learning methods of defect recognition such as Support Vector Machine (SVM) and the Multilayer Perceptron (MLP). It was claimed that the data pre-processing played a small role in the recognition process of DBN as it could learn features from the raw data itself.

Imani et al [11] have developed a novel method to study the influence of process parameters on porosity defects in parts made using the Laser Powder Bed Fusion (L-PBF) process. For that, they were succeeded firstly in mapping the count, size, and location of pores to three L-PBF process parameters namely; the hatch spacing, laser velocity, and laser power, and secondly in monitoring and identifying process environments that are responsible to cause porosity through investigation of in-process layer-by-layer X-ray computed tomography (XCT) images of the build specimen by extracting multifractal and spectral features. The extracted features from the layer-by-layer images as in Fig. 12, for each test part, were subsequently linked to the process parameters using Machine Learning approaches.

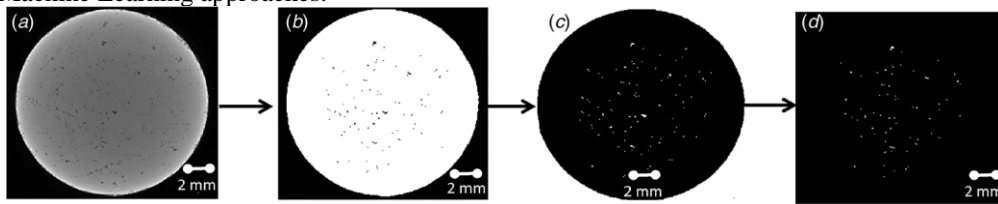


Fig. 12. : (a) XCT scan image of part printed with P -50%, (b) binarization of the XCT scan image of the part, (c) complemented binary image of the XCT scan image, and (d) noise reduced XCT scan image which is used for the spatial distribution analysis

Ti-6Al-4V powder material was used as powder feedstock material. They found that reducing the laser power by 50% leads to nearly a three times increase in the average number of pores, compared to an equivalent percentage increase in hatch spacing, and ten times increase compared to scan velocity. Hence, the control of laser power is most consequential for avoiding porosity. Online visible spectrum photographs of the part were attained as they are built using a still camera. These images were analyzed using multifractal and graph-theoretic approaches and are subsequently used within various machine learning techniques. It was observed that combining multifractal and graph-theoretic analysis leads to as much as a 30% increase in the accuracy of discriminating process conditions compared to using traditional statistical measurements.

Yao et al [12] suggest the use of hybrid AM machines to provide an opportunity to take remedial actions and improve the quality of AM build by considering the uncertainty in transitions from layer to layer along with minimizing the expected cumulative cost through all layers. A hybrid machine can perform subtraction of defective layers along with additive manufacturing. Such corrective actions are different from the adjustment of process parameters. A diagrammatic interpretation of control policy derived from the optimal Constrained Markov Decision Process (CMDP) is depicted in Fig. 13. Rather, they provide an opportunity to repair a layer before going on to the next layer under the condition that process parameters are already set to be optimal.

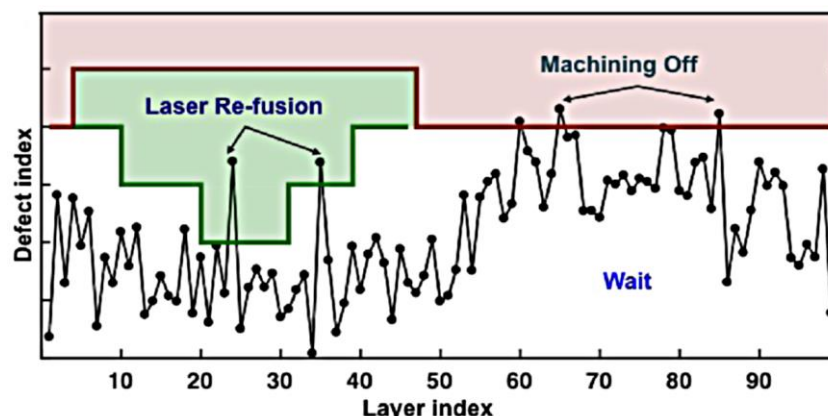


Fig.13. Schematic of hybrid control policy.

Here they claimed to have succeeded in making sequential optimization between two conflicting tasks such as minimizing total energy cost consumed in the manufacturing process and maximizing the quality of finished builds through CMDP.

Montazeri et al [13] have developed and applied a spectral graph-theoretic approach for the in situ determination of the existence of material cross-contamination using in-process photodetector sensors in the L-PBF AM process. Material cross-contamination denotes to trace impurities that may be entered in the powder feedstock used in To find the effects of Material cross-contamination they experimented by contaminating Inconel 625 specimen during L-PBF with tungsten particles. Then converted the raw optical image data into its network graph equivalent, and afterward, extract the spectral graph Fourier coefficients as

proxy signatures to track the process layer-by-layer. The graph Fourier coefficients were extracted for each layer of the material and map out using a Hotelling T^2 control chart depicted in Fig. 15. In which Fig. 14. (a) illustrates the T^2 values of the spectral graph Fourier coefficients with colour coding, red indicates out of control (contaminated) hatches and black indicates in-control hatches. These T^2 values are plotted along the X-Z plane of the part since the position of each hatch is known. Fig (b) depicts the superimposed images of spectral graph T^2 values upon the XCT scan to demarcate the near one-to-one correspondence between the

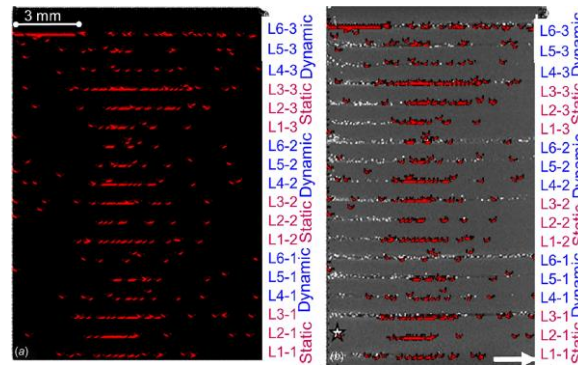


Fig. 14. (a) T^2 values of the spectral graph Fourier coefficients in red colour (b) Superimposed T^2 values and XCT scan image.

two. Spectral graph Fourier coefficients have high fidelity in determining the existence of both tungsten and aluminium contamination. They hypothesized that tracking the signatures learned from the photodetector in the spectral graph domain leads to early and more exact detection of material cross-contamination in L-PBF, compared to the existing Box-Jenkins stochastic delay embedded time series analysis of the signal, such as autoregressive (AR) and autoregressive moving average (ARMA) modelling.

Montazeri et al [14] have adopted a spectral graph theoretic approach to monitoring the L-PBF build state from the data acquired by three types of sensors, namely, a photodetector, high-speed visible camera, and short wave infrared (SWIR) thermal camera depicted schematically in Fig. 15 and compared the results from these sensors in terms of their statistical fidelity in distinguishing between different build conditions.

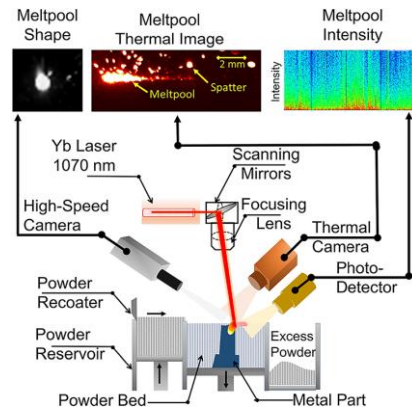


Fig. 15. Schematic diagram of image capturing arrangement

The thermal history of the overhang features from bulk areas of the part is separated as derived signatures in the form of the Eigen spectrum of spectral graph Laplacian matrix. An F-score of 79-95% of this signal analysis technique shows that the statistical accuracy of this technique is higher compared to conventional signal analysis techniques such as neural networks, support vector machines, and linear discriminant analysis with F-score in the range of 40–60. To monitor the L-PBF process, in-process recognizing must be integrated with novel and advanced analytical methods capable of combining data from several sensors compared to existing approaches, such as neural networks that have limitations in accommodating heterogeneous sensors.

Zhang et al [15] have proposed a scheme of hybrid convolutional neural networks (CNNs) for monitoring the powder-bed fusion (PBF) process.

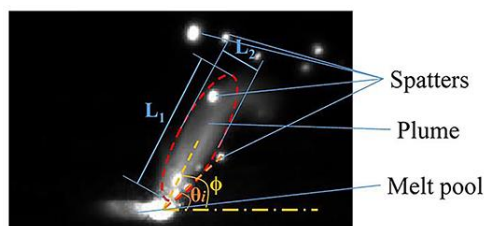


Fig. 16. Melt pool characteristics CNN-1 model ;

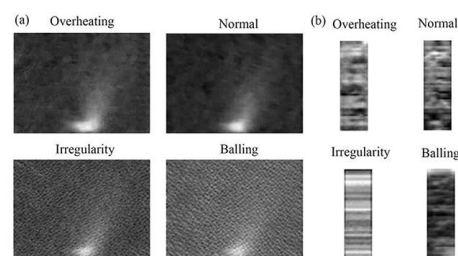


Fig. 17.(a)Extracted features of the four conditions by (b)

CNN-2 model

The suggested algorithm can acquire both the spatial and temporal representative features from the raw images automatically. The raw image data is collected employing a high-speed video camera and data carries the information of melt pool, plume, and spatters as revealed in Fig. 16, which is related to the as-built quality. The raw image data is then fed to hybrid CNNs. Firstly, the CNN-1 model is fully-connected to a multilayer perceptron layer in order to pre-train it independently. The learning features were extracted and rearranged as the input of the CNN-2 model. Then the CNN-2 model was trained based on the sequences of the outputs of the CNN-1 model. The extracted features of the four conditions by the CNN-1 model is shown in Fig. 18(a) and CNN-2 model in Fig. 17 (b). A comparison with traditional deep learning models, such as 3D CNN and LSTM the test accuracy of the proposed method is comparable and the running time is shorter.

Kwon et al [16] have proposed a deep neural network (DNN) that could construct a good regression model to forecast the laser power value from a melt-pool image in Powder Bed Fusion. For that, they used a high-speed camera within a metal AM equipment, that captured nearly 2 Lakhs melt-pool images from coaxial visible light during the AM process as laser power value was changed. Root mean squared error and the coefficient of the determination of CNNs were analyzed to find the best-performed model among various regression models. The best-performed CNN model also provided a higher inference success rate on the Leave-one-out (LOO) evaluation even if the melt-pool images were not in the label sets for deep learning. Therefore, they claimed that the prediction of laser power values from melt-pool images using the proposed model could be used to find the problematic position without destructive tests of AM product.

Kusiak [17] has presented a comparison of CNN with an emerging Machine Learning Technique namely, Generative Adversarial Network (GAN) for its possibilities in Digital Twin Technology. Digital Twin Technology embodies the conjunction of Big Data, AI, and the Internet of Things, where each industrial product will get an active digital representation. As depicted in Fig. 18, a basic generative adversarial network (GAN) consists of two networks, a generator, and a discriminator network, maintaining an adversarial relationship. The advantages of GAN are (1) Ability to model partially labelled data, (2) Training beyond the available data (3) Limited analyst's involvement in training (4) Efficient generation of samples, and (5) High fidelity model. GANs are emerging as powerful tools for unsupervised and semi-supervised learning. Explainable Artificial Intelligence (XAI) [18] is a field within artificial intelligence that aims to address the issue of non-explainability. It focuses on developing techniques and tools to make machine learning models more interpretable and understandable by humans. XAI plays a critical role in bridging the gap between the capabilities of machine learning models and the need for human understanding and trust.

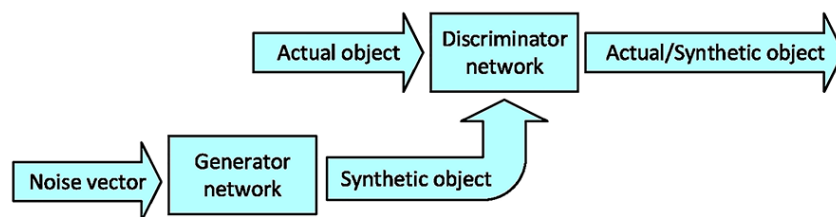


Fig. 18. Schematic of Generative Adversarial Network

V. Conclusion

In this review, the possibilities of various emerging Deep Learning practices such as CNN, DNN, and DBN have been discussed along with the other traditional machine learning techniques. Manufacturing is the latest addition to the application areas of deep neural networks. Both deep learning and traditional machine learning are data-driven artificial intelligence techniques to model process-structure-property-performance (PSPP) relationship in AM. Deep learning has a higher hierarchical structure along with other distinguishing characteristics such as feature learning, model construction, and model training compared to conventional machine learning algorithms. Overall, deep learning has an end-to-end learning framework with the least human intervention, and the parameters in deep learning models are trained together. Besides their paramount advantages, the introduction of deep learning to programmed surface check is still a tough task because it rests heavily on the worth of training samples, mainly the imperfect samples. Also in the potential of Reinforcement Learning in metal AM has not been revealed fully since the number of research papers in this regard is still scarce. Recently the application of deep GAN in manufacturing is a promising development. All the discussed techniques are promising towards the accomplishment of the essential goals of Industry 4.0 such as Agile Manufacturing and Digital Twin technologies.

REFERENCES:

1. Wasmer, K., et al. "In situ quality monitoring in AM using acoustic emission: A reinforcement learning approach." *Journal of Materials Engineering and Performance* 28.2 (2019): 666-672.
2. Gibson, Ian, David W. Rosen, and Brent Stucker. *Additive manufacturing technologies*. Vol. 17. New York: Springer, 2014.
3. Malekipour, Ehsan, and Hazim El-Mounayri. "Defects, process parameters and signatures for online monitoring and control in powder-based additive manufacturing." *Mechanics of Additive and Advanced Manufacturing*, Volume 9. Springer, Cham, 2018. 83-90.
4. Zhang, Bi, Yongtao Li, and Qian Bai. "Defect formation mechanisms in selective laser melting: a review." *Chinese Journal of Mechanical Engineering* 30.3 (2017): 515-527.
5. Grasso, Marco, and Bianca Maria Colosimo. "Process defects and in situ monitoring methods in metal powder bed fusion: a review." *Measurement Science and Technology* 28.4 (2017): 044005.
6. Khorasani, Amir Mahyar, et al. "A survey on mechanisms and critical parameters on solidification of selective laser melting during fabrication of Ti-6Al-4V prosthetic acetabular cup." *Materials & Design* 103 (2016): 348-355.
7. Sames, William J., et al. "The metallurgy and processing science of metal additive manufacturing." *International materials review* 61.5 (2016): 315-360.
8. Kempen, K., et al. "Producing crack-free, high-density M2 Hss parts by selective laser melting: pre-heating the baseplate." *Proceedings of the 24th international solid freeform fabrication symposium*. Laboratory for freeform fabrication, Austin, TX. 2013.
9. Yao, Bing, et al. "Multifractal analysis of image profiles for the characterization and detection of defects in additive manufacturing." *Journal of Manufacturing Science and Engineering* 140.3 (2018).
10. Ye, Dongsun, et al. "Defect detection in selective laser melting technology by acoustic signals with deep belief networks." *The International Journal of Advanced Manufacturing Technology* 96.5-8 (2018): 2791-2801.
11. Imani, Farhad, et al. "Process mapping and in-process monitoring of porosity in Powder Bed Fusion using layerwise optical imaging." *Journal of Manufacturing Science and Engineering* 140.10 (2018).
12. Yao, Bing, and Hui Yang. "Constrained Markov decision process modeling for sequential optimization of additive manufacturing build quality." *IEEE Access* 6 (2018): 54786-54794.
13. Montazeri, Mohammad, et al. "In-process monitoring of material cross-contamination defects in Powder Bed Fusion." *Journal of Manufacturing Science and Engineering* 140.11 (2018).
14. Montazeri, Mohammad, and Prahalada Rao. "Sensor-based build condition monitoring in Powder Bed Fusion additive manufacturing process using a spectral graph-theoretic approach." *Journal of Manufacturing Science and Engineering* 140.9 (2018).
15. Zhang, Yingjie, et al. "Powder-Bed Fusion Process Monitoring by Machine Vision With Hybrid Convolutional Neural Networks." *IEEE Transactions on Industrial Informatics* 16.9 (2019): 5769-5779.
16. Kwon, Ohjung, et al. "A Convolutional Neural Network for Prediction of Laser Power Using Melt-Pool Images in Powder Bed Fusion." *IEEE Access* 8 (2020): 23255-23263.
17. Kusiak, Andrew. "Convolutional and generative adversarial neural networks in manufacturing." *International Journal of Production Research* 58.5 (2020): 1594-1604.
18. Kusiak, Andrew. "Federated explainable artificial intelligence (fXAI): a digital manufacturing perspective." *International journal of production research* (2023): 1-12.